Original Article

Comparison of left ventricular global and segmental strain parameters by cardiovascular magnetic resonance tissue tracking in light-chain cardiac amyloidosis and hypertrophic cardiomyopathy

Fangqing Wang, Xinghua Xu, Qing Wang, Dexin Yu, Lei Lv, Qian Wang^

Department of Radiology, Qilu Hospital of Shandong University, Jinan, China

Contributions: (I) Conception and design: Qian Wang; (II) Administrative support: Qing Wang, D Yu; (III) Provision of study materials or patients: X Xu; (IV) Collection and assembly of data: F Wang, L Lv; (V) Data analysis and interpretation: F Wang; (VI) Manuscript writing: All authors; (VII) Final approval of manuscript: All authors.

Correspondence to: Qian Wang, MD, PhD. Department of Radiology, Qilu Hospital of Shandong University, 107 Wenhuaxi Road, Jinan 250012, China. Email: wangqql@email.sdu.edu.cn.

Background: Apical sparing of left ventricular (LV) strain can occur in light-chain cardiac amyloidosis (AL-CA). We employed indicators of the strain ratio of the apex to base (RAB) and the relative apical sparing of strain (RAS) on the basis of LV global and segmental strain to distinguish AL-CA from hypertrophic cardiomyopathy (HCM).

Methods: In all, 36 AL-CA patients, 37 HCM patients, and 36 healthy controls underwent 3.0 T cardiac magnetic resonance (CMR) examination. We compared LV strain parameters from CMR tissue tracking (CMR-TT), including global and segmental peak radial strain (PRS), peak circumferential strain (PCS), and peak longitudinal strain (PLS); the peak systolic strain rate in radial, circumferential, and longitudinal directions (PSSR_R, PSSR_C, PSSR_L); and the peak diastolic strain rate in radial, circumferential, and longitudinal directions (PDSR_R, PDSR_C, PDSR_L). We also assessed the values of RAB and RAS. Differences in all groups were compared using an independent t-test and a nonparametric rank sum test.

Results: In the comparison of global strain parameters, all the peak strain, systolic, and diastolic peak strain rates of the AL-CA group significantly decreased compared with those of the HCM and healthy control groups (all P<0.001). The values of PSSR in all directions were lower in the AL-CA than in the HCM patients (PSSR_R, P<0.001; PSSR_C, P=0.004; PSSR_L, P=0.010) . In the analysis of segmental strain parameters, all peak strains in the basal segment showed significant differences between the AL-CA and HCM groups (all P<0.001). Some strain rate parameters in the basal segment were also noted to be significantly different (PSSR_R, P<0.001; PSSR_L, P<0.001; PDSR_R, P=0.015; PDSR_C, P=0.020). Both the RAB and RAS of peak strain in all directions showed significant differences between the AL-CA and HCM groups (all P<0.001). The RAB of the radial and circumferential PSSR showed statistical differences between the 2 groups (P<0.001 and P=0.001). The RAS in the radial direction of both the PSSR and PDSR was statistically different (P=0.003 and P=0.012).

Conclusions: The CMR-TT technique can be used to quantitatively compare global and segmental strain differences between AL-CA and HCM. In addition, RAB and RAS are reliable parameters for assessing the apical sparing pattern and thus, for distinguishing AL-CA from HCM.

^ ORCID: 0000-0002-7505-2951.

Keywords: Cardiac magnetic resonance tissue tracking (CMR-TT); light-chain cardiac amyloidosis (AL-CA); hypertrophic cardiomyopathy (HCM); myocardial strain

Submitted Apr 06, 2022. Accepted for publication Sep 14, 2022. Published online Sep 26, 2022.
doi: 10.21037/qims-22-329
View this article at: https://dx.doi.org/10.21037/qims-22-329

Introduction

Amyloidosis is a multisystem disease caused by extracellular accumulation of misfolded proteins and can lead to the loss of normal tissue architecture and function. The most frequent type is light-chain amyloidosis, which can potentially involve any organ. In patients with light-chain cardiac amyloidosis (AL-CA), cardiac involvement can lead to ventricular hypertrophy and impaired systolic and diastolic function (1,2). Owing to the ventricular hypertrophy caused by amyloid deposition, cardiac amyloidosis is often misdiagnosed as hypertrophic cardiomyopathy (HCM). In clinical practice, given the differences in treatment options and the long-term prognosis for these two conditions, it is critically important to differentiate AL-CA from HCM.

Currently, endomyocardial biopsy (EMB) is the gold-standard diagnostic method for AL-CA. However, because of the invasiveness of this method and safety concerns (3), noninvasive diagnostic methods, including echocardiography (ECG), cardiac magnetic resonance (CMR), positron emission tomography (PET), and single-photon emission computed tomography (SPECT), are favored in daily clinical practice (4). Among these, CMR is a versatile approach with high tissue contrast, spatial resolution, and signal-to-noise ratio. CMR also provides detailed information on myocardial structure, function, perfusion, and viability (5,6). In addition, CMR allows disease characterization by late gadolinium enhancement (LGE) and so has important value in the clinical diagnosis of AL-CA. In this regard, a diffuse, delayed enhancement pattern is noted in AL-CA patients, while patchy enhancement is detected in HCM (7,8). However, early AL-CA may not have a typical LGE pattern, and contrast agents may be contraindicated due to renal amyloid deposition. Therefore, to avoid renal injury caused by contrast agents, it is important to use non-contrast agent methods to evaluate AL-CA and distinguish it from HCM.

Currently, the predominant basis for routine clinical assessment of left ventricular (LV) function is left ventricular ejection fraction (LVEF), which reflects the relative change in LV volume (9). To evaluate LV function more comprehensively, it is necessary to trace the characterization of LV mechanics via a noninvasive evaluation of myocardial strain (i.e., the assessment of myocardial strain or intrinsic deformation) (10,11). In this context, strain is defined as the change in fiber length divided by the original length, and it can be quantified according to the orientation of myocardial fibers (radial, circumferential, and longitudinal) (12). Myocardial strain imaging has a high prognostic value for the identification and risk stratification of a wide range of cardiac conditions. Under certain conditions, its decline precedes that of LVEF (13,14). CMR tissue tracking (CMR-TT), an emerging method in myocardial strain analysis, is a simple and robust method used to determine LV strain, which is based on routinely acquired steady-state free precession (SSFP) sequences. Feature-tracking-based software packages have become widely available, allowing the quantification of radial, longitudinal, and circumferential myocardial strains with high levels of accuracy and reproducibility (15,16).

This study aimed to quantify the differences in global and segmental myocardial strain parameters between AL-CA and HCM patients using the CMR-TT technique for the purpose of differential diagnosis.

Methods

Study population

The study was conducted in accordance with the Declaration of Helsinki (as revised in 2013). This retrospective study was approved by the Ethics Committee on Scientific Research of Shandong University Qilu Hospital, and individual consent for this retrospective analysis was waived. We retrospectively analyzed 36 patients with AL-CA between May 2012 and May 2022 (28 men and 8 women, with an average age of 58±10 years). A diagnosis of AL-CA was made based on a biopsy of subcutaneous fat or an involved organ (by Congo red staining under a polarized light microscope with a positive result indicated by apple green birefringence characteristics),

the detection of a monoclonal protein in the serum or urine, and/or a monoclonal population of plasma cells in the bone marrow. Furthermore, the diagnostic criteria for CA were based on the *10th International Symposium on Amyloid and Amyloidosis* (17) as follows: LV wall thickness >12 mm without another known cause as shown by ECG or CMR. We further included 37 patients with HCM (27 men and 10 women, with an average age of 55±8 years). According to the 2020 American Heart Association/American College of Cardiology (AHA/ACC) diagnostic and treatment guidelines for HCM (18), 2-dimensional (2D) ECG or CMR showed that the maximum end-diastolic thickness at any part of the left ventricle was ≥15 mm, and as there was no other cause of myocardial hypertrophy, this could be diagnosed as HCM. In addition, there were 36 age-matched healthy controls (23 men and 13 women, with an average age of 55±6 years). The exclusion criteria were chronic diseases, including cardiovascular disease, diabetes, hypertension (>140/90 mmHg); and a family history of arrhythmia. All patients and controls had glomerular filtration rates >30 mL/min and had no contraindications for magnetic resonance (MR) scanning.

CMR acquisition

All participants underwent magnetic resonance imaging (MRI) scanning using a 3.0-T scanner (GE Signa HDX 3.0 T; GE Healthcare, Chicago, IL, USA) and were placed in the supine position. The scan protocol included stacks of cine images and myocardial LGE (Magnevist; Bayer Healthcare, Wayne, NJ, USA). Images were acquired with retrospective ECG gating during end-expiratory breath holding. Acquisition of 2-, 3-, and 4-chamber long-axis and 9–11 short-axis slices covering the LV was performed. The key parameters were as follows: repetition time (TR)/echo time (TE), 10 ms/1.4 ms; flip angle (FA), 45°; matrix, 256×224; field-of-view (FOV), 350–400 mm; and slice thickness, 8 mm. Myocardial LGE images were acquired with a 2D phase-sensitive inversion-recovery (PSIR) gradient-echo pulse sequence 10 minutes after the intravenous injection of gadolinium. Long- and short-axis slices were acquired at the same position as that for the cine images. Sequence parameters were as follows: TR/TE/FA, 2R/3.1 ms/15°; matrix, 256×224; FOV, 350–400 mm; and slice thickness, 8 mm.

CMR imaging analyses

The SSFP sequence images were imported into Circle CVI[42] software (Circle Cardiovascular Imaging Inc., Calgary, AB, Canada). The parameters were measured by 2 experienced radiologists (with more than 3 years of experience). For the analysis of short- and long-axis images, the software automatically detected the endocardium and manually delimited the epicardial boundary. Papillary muscles and trabeculations were excluded from the myocardial mass and included in the ventricular volume. General CMR parameter measurements and CMR-TT analyses were performed. The CMR-TT analysis method is illustrated in *Figure 1*.

General CMR parameters were exported as Microsoft Excel tables, including the left ventricular end-diastolic volume index (LVEDVi), left ventricular end-systolic volume index (LVESVi), LVEF, left ventricular end-systolic myocardial mass index (LVMi), right ventricular end-diastolic volume index (RVEDVi), right ventricular end-systolic volume index (RVESVi), right ventricular ejection fraction (RVEF), left atrial maximum volume index (LAmaxi), left atrial minimum volume index (LAmini), and left atrial ejection fraction (LAEF).

LV global strain parameters were obtained, including peak radial strain (PRS), peak circumferential strain (PCS), and peak longitudinal strain (PLS). Strain rate parameters were also acquired, including peak systolic strain rate in the radial, circumferential, and longitudinal directions (PSSR_R, PSSR_C, PSSR_L); and peak diastolic strain rate in the radial, circumferential, and longitudinal directions (PDSR_R, PDSR_C, PDSR_L). The LV segmental strain parameters were further measured in different segments of the myocardium (basic, middle, and apical). Two indices were used to evaluate the changing trend of strain from the apex to the base region. The first index was the strain ratio of the apex to base (RAB), calculated as the apical strain/basal strain (19). The other index was the relative apical sparing of strain (RAS), which was calculated as follows: apical strain/(basal strain + middle strain) (20).

Statistical analysis

All statistical analyses were performed using the IBM SPSS for Windows v. 23 (IBM Corp., Armonk, NY, USA) software package. Continuous variables (measurement data) with a normal distribution are presented as the mean ± standard deviation. A *t*-test and nonparametric rank sum test were used for the analysis. All tests were two-sided, and values of $P<0.05$ were considered statistically significant.

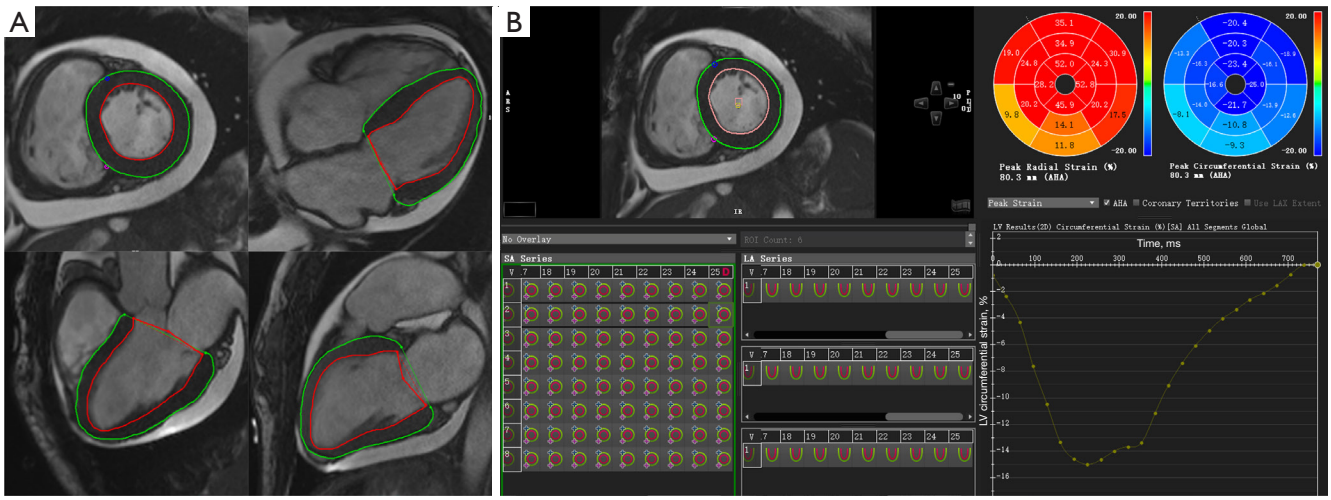

Figure 1 Cardiac magnetic resonance tissue tracking of a patient with light-chain cardiac amyloidosis (female, 50 years old). (A) Endocardial (red) and epicardial (green) contours were drawn in the end-diastolic phase on short-axis, 4-, 3-, and 2-chamber stacked slices. (B) Polar map views and curve graphs were adopted for strain analysis. LV, left ventricular; A, anterior; R, right; S, superior; IR, inferior right; SA, short axis; LA, long axis; LV, left ventricular; AHA, American Heart Association; 2D, two-dimensional.

Results

Baseline characteristics

The comparison of baseline characteristics among AL-CA patients, HCM patients, and healthy controls is shown in *Table 1*. The age and gender of the AL-CA patients, HCM patients, and healthy controls were matched (P=0.334 and P=0.636, respectively). The patients with AL-CA had higher levels of N-terminal pro B-type natriuretic peptide (NT-proBNP) and cardiac troponin-I (cTnI) than did those with HCM (P=0.008 and P=0.009, respectively). The patients with AL-CA also showed characteristics of pleural effusion, pericardial effusion, and low limb conduction voltage on ECG. Although there was no significant difference in the interventricular septum (IVS) thickness between the AL-CA and HCM patients (P=0.248), the LVEF of the patients with AL-CA was significantly lower than that of the patients with HCM (P<0.001). Moreover, two-thirds of the patients with AL-CA were New York Heart Association (NYHA) functional class III to IV, and most of the patients with HCM were NYHA functional class I to II (29/37, 78.3%). The ratio of early LV inflow wave to early diastolic annulus wave (E/e') of the patients AL-CA measured by ECG was significantly higher than that of the patients with HCM (P<0.001).

General CMR parameters

The CMR cine-derived general cardiac parameters are presented in *Table 2*. The AL-CA and HCM patients were matched for LV mass index, with no significant difference between the 2 groups (82.08±23.36 *vs.* 75.30±19.88 g/m^2; P=0.191). In addition, no significant differences were noted between the AL-CA and HCM groups in the LVEDVi (76.30±18.84 *vs.* 78.71±17.31 mL/m^2; P=0.577). The LVEF was significantly lower in the AL-CA than in the HCM group (45.94%±9.76% *vs.* 64.06%±7.84%; P<0.001), while the LVESVi was significantly higher in the AL-CA than in the HCM group (40.82±13.16 *vs.* 28.71±11.04 mL/m^2; P<0.001). Significant differences were observed between the AL-CA and HCM groups in all right ventricular and left atrial functional parameters (RVEDVi, P=0.004; RVESVi, P<0.001; RVEF, P<0.001; LAmaxi, P=0.004; LAmini, P<0.001; LAEF, P<0.001).

LV global and segmental peak strain parameters

The peak strain parameters of the radial, circumferential, and longitudinal directions were acquired automatically and are illustrated in the form of curves and bull's-eye charts (*Figure 1*). As shown in *Table 3*, the global radial, circumferential, and longitudinal peak strains of LV

Table 1 Baseline characteristics of AL-CA patients, HCM patients, and healthy controls

Baseline characteristics	AL-CA (n=36)	HCM (n=37)	Healthy controls (n=36)	P value (AL-CA *vs.* HCM)	P value (all groups)
Age (years)	58±10	55±8	55±6	0.230	0.334
Male	28 (77.78)	27 (72.97)	23 (63.89)	0.634	0.636
BMI (kg/m^2)	24.08±3.11	25.80±2.49	23.65±1.74	0.012	0.003
NT-proBNP (g/L)	7,773.18±7,861.27	763.18±522.68	NA	0.008	NA
cTnI (ng/L)	71.37±136.85	3.42±3.57	NA	0.009	NA
NYHA			NA	<0.001	NA
NYHA I	2 (5.56)	15 (37.84)			
NYHA II	10 (27.78)	14 (35.14)			
NYHA III	14 (38.89)	8 (21.62)			
NYHA IV	10 (27.78)	0 (0)			
Pleural effusion	19 (52.78)	1 (2.70)	0 (0)	<0.001	<0.001
Pericardial effusion	27 (75.00)	2 (5.41)	0 (0)	<0.001	<0.001
Smoker	13 (36.11)	14 (37.84)	12 (33.33)	0.879	0.931
SBP (mmHg)	108±16	127±11	121±6	<0.001	<0.001
DBP (mmHg)	70±9	80±10	83±6	0.001	<0.001
ECG low voltage	14 (38.89)	0 (0)	0 (0)	<0.001	<0.001
Echocardiography					
IVS (mm)	16.67±2.83	17.84±4.61	8.81±1.28	0.248	<0.001
LVEF (%)	43.89±9.38	61.70±13.01	60.93±6.45	<0.001	<0.001
MR	30 (83.33)	7 (18.92)	0 (0)	<0.001	<0.001
TR	29 (80.56)	9 (24.32)	0 (0)	<0.001	<0.001
E/e'	25.16±11.36	9.13±8.77	7.81±1.17	<0.001	<0.001

The values are presented as mean ± standard deviation or number (percentages). AL-CA, light-chain cardiac amyloidosis; HCM, hypertrophic cardiomyopathy; BMI, body mass index; NT-proBNP, N-terminal pro-B-type natriuretic peptide; cTnI, cardiac troponin I; NYHA, New York Heart Association; SBP, systolic blood pressure; DBP, diastolic blood pressure; ECG, echocardiography; IVS, interventricular septum; LVEF, left ventricular ejection fraction; MR, mitral regurgitation; TR, tricuspid regurgitation; E/e', ratio of early left ventricular inflow wave to early diastolic annulus wave.

was significantly decreased in the patients with AL-CA compared with those with HCM (all P<0.001). Significant differences between the AL-CA and HCM patients were also noted in the PSSR (PSSR_R, P<0.001; PSSR_C, P=0.004; PSSR_L, P=0.010). However, no significant differences between the AL-CA and HCM groups were observed in the PDSR (PDSR_R, P=0.378; PDSR_C, P=0.481; PDSR_L, P=0.990).

The segmental strain parameters of the AL-CA and HCM groups were compared (*Table 4*). Significant differences were observed in the basal and middle segments in the PRS and PCS between the 2 groups (all P<0.001). However, no statistically significant differences in the PRS and PCS were noted in the apical segments between the 2 groups (P=0.142 and P=0.266, respectively). The PLSs of the AL-CA and HCM groups showed a significant difference in the basal segment (P<0.001) but not in the middle or apical segments (P=0.121 and P=0.203, respectively). The values of PSSR_R in the basal and middle segments and PSSR_L in the basal segment showed significant differences between the AL-CA and HCM groups (PSSR_R basal, P<0.001; PSSR_R middle, P<0.001;

Table 2 General CMR parameters of AL-CA patients, HCM patients, and healthy controls

General CMR parameters	AL-CA (n=36)	HCM (n=37)	Healthy controls (n=36)	P value (AL-CA *vs.* HCM)	P value (all groups)
LVEDVi (mL/m^2)	76.30±18.84	78.71±17.31	70.09±11.03	0.577	0.201
LVESVi (mL/m^2)	40.82±13.16	28.71±11.04	25.52±6.47	<0.001	<0.001
LVEF (%)	45.94±9.76	64.06±7.84	64.1±7.53	<0.001	<0.001
LVMi (g/m^2)	82.08±23.36	75.30±19.88	43.18±9.34	0.191	<0.001
RVEDVi (mL/m^2)	81.44±17.20	70.18±14.05	71.82±12.51	0.004	<0.001
RVESVi (mL/m^2)	45.55±14.78	25.63±8.66	28.44±6.46	<0.001	<0.001
RVEF (%)	44.46±10.01	63.53±8.13	60.57±5.77	<0.001	<0.001
LAmaxi (mL/m^2)	57.87±20.47	44.23±18.18	33.74±10.50	0.004	<0.001
LAmini (mL/m^2)	41.34±17.88	21.58±12.44	13.02±6.31	<0.001	<0.001
LAEF (%)	28.38±13.55	53.51±10.32	62.31±9.43	<0.001	<0.001

The values are presented as mean ± standard deviation. CMR, cardiac magnetic resonance; AL-CA, light-chain cardiac amyloidosis; HCM, hypertrophic cardiomyopathy; LVEDVi, left ventricular end-diastolic volume index; LVESVi, left ventricular end-systolic volume index; LVEF, left ventricular ejection fraction; LVMi, left ventricular myocardial mass index; RVEDVi, right ventricular end-diastolic volume index; RVESVi, right ventricular end-systolic volume index; RVEF, right ventricular ejection fraction; LAmaxi, left atrial maximum volume index; LAmini, left atrial minimum volume index; LAEF, left atrial ejection fraction.

Table 3 Global LV strain comparison of AL-CA patients, HCM patients, and healthy controls

LV strain	AL-CA (n=36)	HCM (n=37)	Healthy controls (n=36)	P value (AL-CA *vs.* HCM)	P value (all groups)
PRS (%)	19.85±5.74	30.93±7.14	36.96±7.93	<0.001	<0.001
PCS (%)	−13.16±2.70	−17.67±2.56	−20.3±2.28	<0.001	<0.001
PLS (%)	−7.21±4.35	−11.81±3.40	−15.7±2.79	<0.001	<0.001
PSSR_R (1/s)	1.28±0.71	2.09±0.81	2.16±0.57	<0.001	<0.001
PSSR_C (1/s)	−0.87±0.40	−1.11±0.27	−1.09±0.19	0.004	<0.001
PSSR_L (1/s)	−0.50±0.51	−0.74±0.24	−0.86±0.27	0.010	<0.001
PDSR_R (1/s)	−1.25±1.40	−1.50±0.97	−2.19±0.72	0.378	<0.001
PDSR_C (1/s)	0.77±0.69	0.85±0.27	1.97±0.22	0.481	<0.001
PDSR_L (1/s)	0.52±0.60	0.52±0.29	0.79±0.16	0.990	<0.001

The values are presented as mean ± standard deviation. LV, left ventricle; AL-CA, light-chain cardiac amyloidosis; HCM, hypertrophic cardiomyopathy; PRS, peak radial strain; PCS, peak circumferential strain; PLS, peak longitudinal strain; PSSR, peak systolic strain rate; PDSR, peak diastolic strain rate; R, radial; C, circumferential; L, longitudinal.

PSSR_L basal, P<0.001). There were no significant differences in the other PSSR parameters between the 2 groups. Among the segmental PDSR parameters, only PDSR_R and PDSR_C in the basal segments showed significant differences between the AL-CA and HCM groups (PDSR_R basal, P=0.015; and PDSR_C basal, P=0.020). No statistical differences in any of the apical strain parameters were observed (all P>0.05).

RAB and RAS analysis

The RAB and RAS were used to depict the apex-sparing features of patients with AL-CA (*Table 5*). Both RAB and RAS in the radial, circumferential, and longitudinal

Table 4 Segmental LV strain parameters of AL-CA patients, HCM patients, and healthy controls

LV strain	AL-CA (n=36)	HCM (n=37)	Healthy controls (n=36)	P value (AL-CA *vs.* HCM)	P value (all groups)
PRS (%)					
Basal	17.17±7.37	35.82±11.37	41.71±10.82	<0.001	<0.001
Middle	20.00±6.52	28.17±7.38	30.82±6.19	<0.001	<0.001
Apical	31.81±11.59	36.28±13.86	48.34±15.36	0.142	<0.001
PCS (%)					
Basal	−11.62±3.48	−18.80±3.33	−21.5±2.67	<0.001	<0.001
Middle	−13.35±2.95	−16.96±2.91	−18.5±2.15	<0.001	<0.001
Apical	−17.96±3.87	−19.00±3.99	−23.1±3.57	0.266	<0.001
PLS (%)					
Basal	−8.04±7.60	−19.33±4.11	−23.1±3.82	<0.001	<0.001
Middle	−4.99±5.92	−7.31±6.64	−10.1±4.60	0.121	<0.001
Apical	−8.04±7.04	−9.73±3.60	−13.70±3.18	0.203	<0.001
PSSR_R (1/s)					
Basal	1.28±0.65	2.31±0.75	2.36±0.72	<0.001	<0.001
Middle	1.27±0.83	2.06±0.89	1.84±0.48	<0.001	<0.001
Apical	2.53±2.21	2.85±1.35	3.10±1.33	0.463	0.082
PSSR_C (1/s)					
Basal	−0.93±0.37	−1.11±0.49	−1.16±0.22	0.077	0.001
Middle	−0.90±0.52	−1.10±0.33	−1.01±0.18	0.051	0.054
Apical	−1.54±0.96	−1.40±0.40	−1.36±0.40	0.441	0.790
PSSR_L (1/s)					
Basal	−0.63±0.98	−1.30±0.41	−1.41±0.43	<0.001	<0.001
Middle	−0.51±0.61	−0.47±0.74	−0.72±0.34	0.809	0.078
Apical	−0.72±0.74	−0.89±0.57	−0.94±0.29	0.275	0.208
PDSR_R (1/s)					
Basal	−1.09±1.54	−2.38±2.68	−2.98±−0.98	0.015	<0.001
Middle	−1.07±2.00	−1.43±1.00	−1.95±0.70	0.341	<0.001
Apical	−2.03±3.29	−2.06±1.80	−3.05±1.84	0.957	0.001
PDSR_C (1/s)					
Basal	0.66±0.75	1.08±0.75	1.15±0.26	0.020	<0.001
Middle	0.82±0.87	0.87±0.45	1.09±0.25	0.783	0.005
Apical	1.04±1.53	1.11±0.65	1.40±0.35	0.809	0.004

Table 4 (*continued*)

Table 4 (*continued*)

LV strain	AL-CA (n=36)	HCM (n=37)	Healthy controls (n=36)	P value (AL-CA *vs.* HCM)	P value (all groups)
PDSR_L (1/s)					
Basal	0.87±1.24	1.08±0.39	1.26±0.27	0.341	<0.001
Middle	0.39±0.91	0.40±0.49	0.71±0.23	0.959	<0.001
Apical	0.61±1.07	0.57±0.64	0.85±0.24	0.838	0.022

The values are presented as mean ± standard deviation. LV, left ventricle; AL-CA, light-chain cardiac amyloidosis; HCM, hypertrophic cardiomyopathy; PRS, peak radial strain; PCS, peak circumferential strain; PLS, peak longitudinal strain; PSSR, peak systolic strain rate; PDSR, peak diastolic strain rate; R, radial; C, circumferential; L, longitudinal.

Table 5 Comparison of RAB and RAS of AL-CA patients, HCM patients, and healthy controls

Variables	AL-CA (n=36)	HCM (n=37)	Healthy controls (n=36)	P value (AL-CA *vs.* HCM)	P value (all groups)
$RAB_{peak\ strain}$ (%)					
Radial	2.08±0.96	1.08±0.44	1.19±0.36	<0.001	<0.001
Circumferential	1.66±0.55	1.03±0.27	1.08±0.18	<0.001	<0.001
Longitudinal	0.90±0.56	0.52±0.23	0.61±0.16	<0.001	<0.001
$RAB_{peak\ systolic\ strain\ rate}$ (%)					
Radial	2.24±1.70	1.26±0.50	1.37±0.52	<0.001	<0.001
Circumferential	1.80±0.98	1.15±0.50	1.20±0.35	0.001	<0.001
Longitudinal	0.83±0.55	0.74±0.66	0.69±0.15	0.601	0.019
$RAB_{peak\ diastolic\ strain\ rate}$ (%)					
Radial	1.18±3.60	1.05±0.91	1.08±0.40	0.908	0.002
Circumferential	0.94±2.41	1.25±0.69	1.25±0.29	0.391	0.216
Longitudinal	0.68±0.93	0.64±0.57	0.71±0.28	0.519	0.208
$RAS_{peak\ strain}$ (%)					
Radial	18.82±7.17	37.13±11.26	43.28±10.77	<0.001	<0.001
Circumferential	−10.25±3.63	−17.67±3.43	−20.27±2.72	<0.001	<0.001
Longitudinal	−6.48±7.42	−17.85±4.55	−21.66±3.85	<0.001	<0.001
$RAS_{peak\ systolic\ strain\ rate}$ (%)					
Radial	2.86±1.52	3.73±0.81	4.06±0.86	0.003	<0.001
Circumferential	0.44±1.12	0.19±0.62	0.19±0.45	0.236	0.007
Longitudinal	0.65±1.37	0.83±3.77	0.06±0.75	0.788	0.014
$RAS_{peak\ diastolic\ strain\ rate}$ (%)					
Radial	0.65±2.60	−1.11±3.14	−1.32±1.17	0.012	<0.001
Circumferential	2.11±1.55	2.33±1.00	2.47±0.42	0.478	0.096
Longitudinal	1.81±1.83	2.12±1.46	2.56±0.51	0.437	0.118

The values are presented as mean ± standard deviation. AL-CA, light-chain cardiac amyloidosis; HCM, hypertrophic cardiomyopathy; RAB, strain ratio of apex to base; RAS, relative apical sparing of strain.

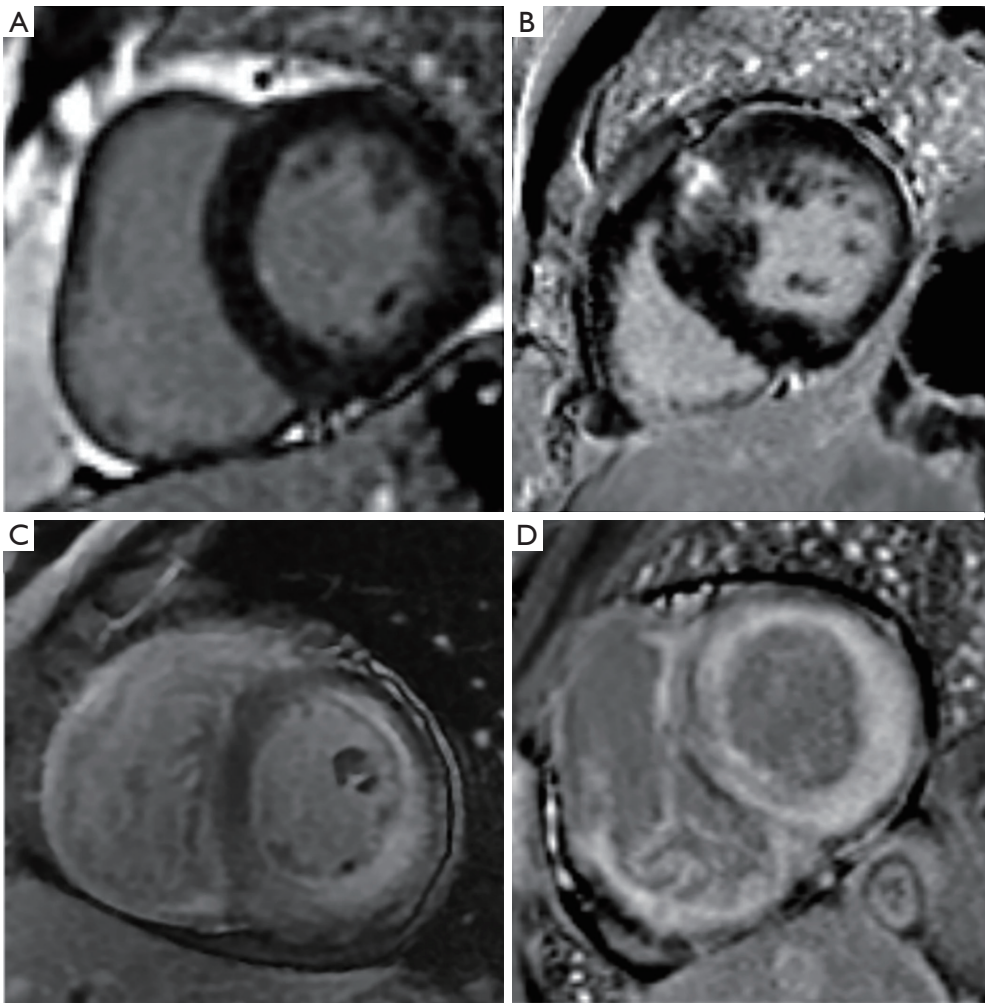

Figure 2 Myocardial LGE patterns of AL-CA, patients with HCM, and healthy controls. (A) A lack of myocardial LGE in healthy controls. (B) Intramyocardial patchy LGE in patients with HCM. (C,D) Subendocardial and transmural pattern LGE in patients with AL-CA. LGE, late gadolinium enhancement; AL-CA, light-chain patients with cardiac amyloidosis; HCM, hypertrophic cardiomyopathy.

directions of peak strain showed significant differences between the AL-CA and HCM groups (all P<0.001). Statistical differences were noted in the RAB of the PSSR_R and PSSR_C (P<0.001 and P=0.001, respectively). The RAS of both the PSSR_R and PDSR_R were significantly different between the 2 groups (P=0.003 and P=0.012, respectively). No statistical differences were noted in the other RAB or RAS parameters between the 2 groups.

LV myocardial LGE pattern

All 36 patients with AL-CA had varying degrees of myocardial LGE, including 17 with subendocardial LGE and 19 with transmural LGE. Among the 37 patients with HCM, 33 patients showed patchy LGE in the hypertrophic myocardium, including 11 cases with single-segment involvement and 22 cases with multiple-segment involvement. Myocardial LGE was not observed in any of the healthy controls (*Figure 2*).

Discussion

CMR provides multiple functional indices for cardiomyopathy. With the CMR-TT technique, the strain parameters in the radial, circumferential, and longitudinal directions can be quantified, and both global and segmental strain

parameters can be further evaluated (21). The normal range of LV global and segmental strain based on a large, healthy population has been reported (22). In this study, we compared the differences in LV peak strain, PSSR, and PDSR in 3 directions between patients with AL-CA and those with HCM. We also assessed the segmental strain change from base to apex to obtain more comprehensive myocardial motion information from the perspective of biomechanics.

The subendocardial myocardium parallel to the long axis of the heart mainly affects longitudinal strain, the oblique subepicardial myocardium mainly contributes to circumferential strain, and the radial strain consists of the combined action of all myocardial layers (23). In patients with AL-CA, amyloid is deposited in the subendocardial myocardium at an early stage of disease, which mainly affects long-axis strain. Therefore, a decrease in LV long-axis strain is a classic index for the evaluation of myocardial amyloidosis (4,24). With disease progression, the extent of myocardial involvement expands, and transmural injury occurs in the late stage of disease. As a result, the reduction in PRS and PCS gradually becomes obvious (16). Previous evaluations of PRS and PCS in patients with amyloidosis concluded that PRS and PCS also have high diagnostic efficacy for amyloidosis (19,25). Our study showed that peak strain in 3 directions and PSSR in the radial and circumferential directions were effective in the differential diagnosis of AL-CA and HCM. The underlying reason is that amyloid deposition in patients with AL-CA involves the midmyocardium or even the subepicardial myocardium.

Myocardial amyloidosis is a type of restricted cardiomyopathy characterized by abnormal LV filling and restricted relaxation (26). Patients with HCM also present with LV diastolic dysfunction due to abnormal hypertrophy and the disordered arrangement of cardiomyocytes, myocardial interstitial fibrosis, and a consequent decrease in myocardial compliance (27). While the gold standard for the measurement of LV diastolic function is cardiac catheterization, its clinical application is limited due to its invasiveness. ECG has become the optimal choice and can provide multiple indices, such as diastolic mitral flow characteristics, pulmonary venous flow pattern, and the Tei index (28,29). Using the CMR-TT technique, a series of LV systolic and diastolic strain parameters can be obtained in one step (30-32).

In our study, although the LVEF of patients with HCM was within the normal range, the value of PDSR in 3 directions was lower than that in the healthy controls, which confirmed that diastolic function was impaired earlier than systolic function in patients with HCM. Moreover, none of the PDSR indices in the AL-CA or HCM groups were significantly different, indicating that global LV diastolic dysfunction was similar between the 2 groups. However, segmental strain analysis showed that the radial and circumferential PDSR values in the basal segment of the patients with AL-CA were significantly lower than in those with HCM, suggesting severe basal segmental diastolic impairments in the AL-CA group.

A variety of myopathic processes, such as amyloidosis, HCM, and hypertension, can lead to LV hypertrophy and a reduction in global strain parameters. Therefore, the specificity of this technique is limited. Studies based on ECG and MRI found a characteristic apical-sparing pattern in patients with AL-CA (33,34), in which the apical longitudinal strain was relatively normal, whereas the basal and middle strains were reduced, suggesting that amyloid deposition in the apical region is less than that in the basal region. Therefore, the resistance to deformation may be lower (35). The segmental strain analysis of our study showed that the basal segmental strain parameters of the AL-CA group were lower than those of the HCM group, except for the circumferential PSSR and longitudinal PDSR, suggesting that amyloid lesions could impair motor function more significantly in the basal segment.

In evaluating the difference between basal and apical strains more explicitly, the RAB and the RAS have been applied as sensitive indicators (36). The RAB is simple to calculate and mainly involves the evaluation of the difference between the basal and apical strains (37). By contrast, the middle segmental strain can be included in the RAS calculation to make the evaluation more comprehensive and reasonable (38). In contrast to similar studies (34,37), we added the evaluation of the RAB and the RAS of the radial and circumferential strain parameters. Our results indicated that these parameters had the same value as the longitudinal strain parameters in the depiction of the apical sparing pattern of AL-CA. Notably, the RAB and the RAS of the peak radial systolic strain rate demonstrated good diagnostic efficacy and verified the value of the radial strain parameter in distinguishing between AL-CA and HCM (39).

Our study had several limitations. First, it employed retrospective cohort design with a small sample size. Second, the classification of HCM was not performed, which might have led to discrepancy upon application to all

patients with HCM. Third, not all patients with amyloidosis underwent EMB. However, additional criteria were adopted to confirm cardiac involvement.

Conclusions

The CMR-TT technique can be used to quantitatively compare the global and segmental strain differences between AL-CA and HCM. In addition, the RAB and the RAS are reliable parameters for the assessment of the apical sparing pattern in distinguishing AL-CA from HCM.

Acknowledgments

Funding: This work was supported by the Key Research and Development Projects of Shandong Province, China (No. 2018GSF118239).

Footnote

Conflicts of Interest: All authors have completed the ICMJE uniform disclosure form (available at https://qims.amegroups.com/article/view/10.21037/qims-22-329/coif). The authors have no conflicts of interest to declare.

Ethical Statement: The authors are accountable for all aspects of the work in ensuring that questions related to the accuracy or integrity of any part of the work are appropriately investigated and resolved. The study was conducted in accordance with the Declaration of Helsinki (as revised in 2013). This retrospective study was approved by the Ethics Committee on Scientific Research of Shandong University Qilu Hospital, and individual consent for this retrospective analysis was waived.

References

1. Mankad AK, Sesay I, Shah KB. Light-chain cardiac amyloidosis. Curr Probl Cancer 2017;41:144-56.
2. Liu H, Bai P, Xu HY, Li ZL, Xia CC, Zhou XY, Gong LG, Guo YK. Distinguishing Cardiac Amyloidosis and Hypertrophic Cardiomyopathy by Thickness and Myocardial Deformation of the Right Ventricle. Cardiol Res Pract 2022;2022:4364279.
3. Kuetting DL, Homsi R, Sprinkart AM, Luetkens J, Thomas DK, Schild HH, Dabir D. Quantitative assessment of systolic and diastolic function in patients with LGE negative systemic amyloidosis using CMR. Int J Cardiol 2017;232:336-41.
4. Williams LK, Forero JF, Popovic ZB, Phelan D, Delgado D, Rakowski H, Wintersperger BJ, Thavendiranathan P. Patterns of CMR measured longitudinal strain and its association with late gadolinium enhancement in patients with cardiac amyloidosis and its mimics. J Cardiovasc Magn Reson 2017;19:61.
5. Saeed M, Liu H, Liang CH, Wilson MW. Magnetic resonance imaging for characterizing myocardial diseases. Int J Cardiovasc Imaging 2017;33:1395-414.
6. Ibrahim el-SH. Myocardial tagging by cardiovascular magnetic resonance: evolution of techniques--pulse sequences, analysis algorithms, and applications. J Cardiovasc Magn Reson 2011;13:36.
7. Zhao L, Tian Z, Fang Q. Diagnostic accuracy of cardiovascular magnetic resonance for patients with suspected cardiac amyloidosis: a systematic review and meta-analysis. BMC Cardiovasc Disord 2016;16:129.
8. Edelman RR. Contrast-enhanced MR imaging of the heart: overview of the literature. Radiology 2004;232:653-68.
9. Schuster A, Hor KN, Kowallick JT, Beerbaum P, Kutty S. Cardiovascular Magnetic Resonance Myocardial Feature Tracking: Concepts and Clinical Applications. Circ Cardiovasc Imaging 2016;9:e004077.
10. Amzulescu MS, De Craene M, Langet H, Pasquet A, Vancraeynest D, Pouleur AC, Vanoverschelde JL, Gerber BL. Myocardial strain imaging: review of general principles, validation, and sources of discrepancies. Eur Heart J Cardiovasc Imaging 2019;20:605-19.
11. Halliday BP, Senior R, Pennell DJ. Assessing left ventricular systolic function: from ejection fraction to strain analysis. Eur Heart J 2021;42:789-97.
12. Liu J, Li Y, Cui Y, Cao Y, Yao S, Zhou X, Wetzl J, Zeng W, Shi H. Quantification of myocardial strain in patients with isolated left ventricular non-compaction and healthy subjects using deformable registration algorithm: comparison with feature tracking. BMC Cardiovasc Disord

2020;20:400.
13. Bucius P, Erley J, Tanacli R, Zieschang V, Giusca S, Korosoglou G, Steen H, Stehning C, Pieske B, Pieske-Kraigher E, Schuster A, Lapinskas T, Kelle S. Comparison of feature tracking, fast-SENC, and myocardial tagging for global and segmental left ventricular strain. ESC Heart Fail 2020;7:523-32.
14. Faganello G, Collia D, Furlotti S, Pagura L, Zaccari M, Pedrizzetti G, Di Lenarda A. A new integrated approach to cardiac mechanics: reference values for normal left ventricle. Int J Cardiovasc Imaging 2020;36:2173-85.
15. Dobrovie M, Barreiro-Pérez M, Curione D, Symons R, Claus P, Voigt JU, Bogaert J. Inter-vendor reproducibility and accuracy of segmental left ventricular strain measurements using CMR feature tracking. Eur Radiol 2019;29:6846-57.
16. Wan K, Sun J, Yang D, Liu H, Wang J, Cheng W, Zhang Q, Zeng Z, Zhang T, Greiser A, Jolly MP, Han Y, Chen Y. Left Ventricular Myocardial Deformation on Cine MR Images: Relationship to Severity of Disease and Prognosis in Light-Chain Amyloidosis. Radiology 2018;288:73-80.
17. Gertz MA, Comenzo R, Falk RH, Fermand JP, Hazenberg BP, Hawkins PN, Merlini G, Moreau P, Ronco P, Sanchorawala V, Sezer O, Solomon A, Grateau G. Definition of organ involvement and treatment response in immunoglobulin light chain amyloidosis (AL): a consensus opinion from the 10th International Symposium on Amyloid and Amyloidosis, Tours, France, 18-22 April 2004. Am J Hematol 2005;79:319-28.
18. Ommen SR, Mital S, Burke MA, Day SM, Deswal A, Elliott P, Evanovich LL, Hung J, Joglar JA, Kantor P, Kimmelstiel C, Kittleson M, Link MS, Maron MS, Martinez MW, Miyake CY, Schaff HV, Semsarian C, Sorajja P. 2020 AHA/ACC Guideline for the Diagnosis and Treatment of Patients With Hypertrophic Cardiomyopathy: Executive Summary: A Report of the American College of Cardiology/American Heart Association Joint Committee on Clinical Practice Guidelines. Circulation 2020;142:e533-57.
19. Jung HN, Kim SM, Lee JH, Kim Y, Lee SC, Jeon ES, Yong HS, Choe YH. Comparison of tissue tracking assessment by cardiovascular magnetic resonance for cardiac amyloidosis and hypertrophic cardiomyopathy. Acta Radiol 2020;61:885-93.
20. Phelan D, Collier P, Thavendiranathan P, Popović ZB, Hanna M, Plana JC, Marwick TH, Thomas JD. Relative apical sparing of longitudinal strain using two-dimensional speckle-tracking echocardiography is both sensitive and specific for the diagnosis of cardiac amyloidosis. Heart 2012;98:1442-8.
21. Claus P, Omar AMS, Pedrizzetti G, Sengupta PP, Nagel E. Tissue Tracking Technology for Assessing Cardiac Mechanics: Principles, Normal Values, and Clinical Applications. JACC Cardiovasc Imaging 2015;8:1444-60.
22. Qu YY, Paul J, Li H, Ma GS, Buckert D, Rasche V. Left ventricular myocardial strain quantification with two- and three-dimensional cardiovascular magnetic resonance based tissue tracking. Quant Imaging Med Surg 2021;11:1421-36.
23. Beyhoff N, Lohr D, Foryst-Ludwig A, Klopfleisch R, Brix S, Grune J, Thiele A, Erfinanda L, Tabuchi A, Kuebler WM, Pieske B, Schreiber LM, Kintscher U. Characterization of Myocardial Microstructure and Function in an Experimental Model of Isolated Subendocardial Damage. Hypertension 2019;74:295-304.
24. Quarta CC, Solomon SD, Uraizee I, Kruger J, Longhi S, Ferlito M, Gagliardi C, Milandri A, Rapezzi C, Falk RH. Left ventricular structure and function in transthyretin-related versus light-chain cardiac amyloidosis. Circulation 2014;129:1840-9.
25. Oda S, Utsunomiya D, Nakaura T, Yuki H, Kidoh M, Morita K, Takashio S, Yamamuro M, Izumiya Y, Hirakawa K, Ishida T, Tsujita K, Ueda M, Yamashita T, Ando Y, Hata H, Yamashita Y. Identification and Assessment of Cardiac Amyloidosis by Myocardial Strain Analysis of Cardiac Magnetic Resonance Imaging. Circ J 2017;81:1014-21.
26. Chacko L, Martone R, Cappelli F, Fontana M. Cardiac Amyloidosis: Updates in Imaging. Curr Cardiol Rep 2019;21:108.
27. Geske JB, Ommen SR, Gersh BJ. Hypertrophic Cardiomyopathy: Clinical Update. JACC Heart Fail 2018;6:364-75.
28. Su HM, Lin TH, Voon WC, Lee KT, Chu CS, Yen HW, Lai WT, Sheu SH. Correlation of Tei index obtained from tissue Doppler echocardiography with invasive measurements of left ventricular performance. Echocardiography 2007;24:252-7.
29. Nagueh SF, Smiseth OA, Appleton CP, Byrd BF 3rd, Dokainish H, Edvardsen T, Flachskampf FA, Gillebert TC, Klein AL, Lancellotti P, Marino P, Oh JK, Alexandru Popescu B, Waggoner AD; Houston, Texas; Oslo, Norway; Phoenix, Arizona; Nashville, Tennessee; Hamilton, Ontario, Canada; Uppsala, Sweden; Ghent and Liège, Belgium; Cleveland, Ohio; Novara, Italy; Rochester, Minnesota; Bucharest, Romania; and St. Louis, Missouri. Recommendations for the Evaluation of Left Ventricular

Diastolic Function by Echocardiography: An Update from the American Society of Echocardiography and the European Association of Cardiovascular Imaging. Eur Heart J Cardiovasc Imaging 2016;17:1321-60.
30. Chamsi-Pasha MA, Zhan Y, Debs D, Shah DJ. CMR in the Evaluation of Diastolic Dysfunction and Phenotyping of HFpEF: Current Role and Future Perspectives. JACC Cardiovasc Imaging 2020;13:283-96.
31. Ng MY, Tong X, He J, Lin Q, Luo L, Chen Y, Shen XP, Wan EYF, Yan AT, Yiu KH. Feature tracking for assessment of diastolic function by cardiovascular magnetic resonance imaging. Clin Radiol 2020;75:321.e1-321.e11.
32. Zhu L, Gu S, Wang Q, Zhou X, Wang S, Fu C, Yang W, Wetzl J, Yan F. Left ventricular myocardial deformation: a study on diastolic function in the Chinese male population and its relationship with fat distribution. Quant Imaging Med Surg 2020;10:634-45.
33. Fikrle M, Palecek T, Marek J, Kuchynka P, Linhart A. Simplified apical four-chamber view evaluation of relative apical sparing of longitudinal strain in diagnosing AL amyloid cardiomyopathy. Echocardiography 2018;35:1764-71.
34. Bravo PE, Fujikura K, Kijewski MF, Jerosch-Herold M, Jacob S, El-Sady MS, Sticka W, Dubey S, Belanger A, Park MA, Di Carli MF, Kwong RY, Falk RH, Dorbala S. Relative Apical Sparing of Myocardial Longitudinal Strain Is Explained by Regional Differences in Total Amyloid Mass Rather Than the Proportion of Amyloid Deposits. JACC Cardiovasc Imaging 2019;12:1165-73.
35. Ternacle J, Bodez D, Guellich A, Audureau E, Rappeneau S, Lim P, Radu C, Guendouz S, Couetil JP, Benhaiem N, Hittinger L, Dubois-Randé JL, Plante-Bordeneuve V, Mohty D, Deux JF, Damy T. Causes and Consequences of Longitudinal LV Dysfunction Assessed by 2D Strain Echocardiography in Cardiac Amyloidosis. JACC Cardiovasc Imaging 2016;9:126-38.
36. Dahl Pedersen AL, Povlsen JA, Dybro A, Clemmensen TS, Larsen AH, Ladefoged B, Poulsen SH. Prevalence and Prognostic Implications of Increased Apical-to-Basal Strain Ratio in Patients with Aortic Stenosis Undergoing Transcatheter Aortic Valve Replacement. J Am Soc Echocardiogr 2020;33:1465-73.
37. Dohy Z, Szabo L, Pozsonyi Z, Csecs I, Toth A, Suhai FI, Czimbalmos C, Szucs A, Kiss AR, Becker D, Merkely B, Vago H. Potential clinical relevance of cardiac magnetic resonance to diagnose cardiac light chain amyloidosis. PLoS One 2022;17:e0269807.
38. Usuku H, Takashio S, Yamamoto E, Kinoshita Y, Nishi M, Oike F, Marume K, Hirakawa K, Tabata N, Oda S, Misumi Y, Ueda M, Kawano H, Kaikita K, Matsushita K, Ando Y, Matsui H, Tsujita K. Usefulness of relative apical longitudinal strain index to predict positive 99m Tc-labeled pyrophosphate scintigraphy findings in advanced-age patients with suspected transthyretin amyloid cardiomyopathy. Echocardiography 2020;37:1774-83.
39. Pandey T, Alapati S, Wadhwa V, Edupuganti MM, Gurram P, Lensing S, Jambhekar K. Evaluation of Myocardial Strain in Patients With Amyloidosis Using Cardiac Magnetic Resonance Feature Tracking. Curr Probl Diagn Radiol 2017;46:288-94.

Cite this article as: Wang F, Xu X, Wang Q, Yu D, Lv L, Wang Q. Comparison of left ventricular global and segmental strain parameters by cardiovascular magnetic resonance tissue tracking in light-chain cardiac amyloidosis and hypertrophic cardiomyopathy. Quant Imaging Med Surg 2023;13(1):449-461. doi: 10.21037/qims-22-329

